Vg1RBP phosphorylation by Erk2 MAP kinase correlates with the cortical release of Vg1 mRNA during meiotic maturation of *Xenopus* oocytes

ANNA GIT,[1,4] RACHEL ALLISON,[1,5] EUSEBIO PERDIGUERO,[2,6] ANGEL R. NEBREDA,[2] EVELYN HOULISTON,[3] and NANCY STANDART[1]

[1]Department of Biochemistry, University of Cambridge, Cambridge CB2 1GA, United Kingdom
[2]Spanish National Cancer Center (CNIO), Madrid 28029, Spain
[3]Developmental Biology Unit 7009, Universite Pierre et Marie Curie (Paris VI), and Centre National de la Recherche (CNRS), Observatoire Oceanologique, 06320 Villefranche-sur-mer, France

ABSTRACT

Xenopus Vg1RBP is a member of the highly conserved IMP family of four KH-domain RNA binding proteins, with roles in RNA localization, translational control, RNA stability, and cell motility. Vg1RBP has been implicated in localizing Vg1 mRNAs to the vegetal cortex during oogenesis, in a process mediated by microtubules and microfilaments, and in migration of neural crest cells in embryos. Using *c-mos* morpholino, kinase inhibitors, and constitutely active recombinant kinases we show that Vg1RBP undergoes regulated phosphorylation by Erk2 MAPK during meiotic maturation, on a single residue, S402, located between the KH2 and KH3 domains. Phosphorylation temporally correlates with the release of Vg1 mRNA from its tight cortical association, assayed in lysates in physiological salt buffers, but does not affect RNA binding, nor self-association of Vg1RBP. U0126, a MAP kinase inhibitor, prevents Vg1RBP cortical release and Vg1 mRNA solubilization in meiotically maturing eggs, while injection of MKK6-DD, a constitutively activated MAP kinase kinase, promotes the release of both Vg1RBP and Vg1 mRNA from insoluble cortical structures. We propose that Erk2 MAP kinase phosphorylation of Vg1RBP regulates the protein:protein-mediated association of Vg1 mRNP with the cytoskeleton and/or ER. Since the MAP kinase site in Vg1RBP is conserved in several IMP homologs, this modification also has important implications for the regulation of IMP proteins in somatic cells.

Keywords: IMP; VICKZ; RNA-binding; KH domain; RNA localization

INTRODUCTION

Vg1RBP is a member of an important family of regulatory RNA-binding proteins which includes ZBP-1, CRD-BP, and KOC proteins, known as IMP/VICKZ proteins (for review, see Yisraeli 2005). Mammals possess three highly conserved IMP proteins (IMP1-3) which are differentially expressed, while in *Xenopus*, Vg1RBP (also known as Vera; IMP3) is the sole representative of this family. The vertebrate proteins apparently contain six RNA-binding domains, with two tandem RRM (RNA recognition motifs) in the N terminus followed by four tandem KH (hnRNP K-homologous) domains. However, RNA-binding has not been observed for either RRM, and moreover, *Drosophila* IMP lacks these domains altogether. Instead, the four KH domains, organized as two didomains, are responsible for RNA-binding, as well as for self-association (Git and Standart 2002; Nielsen et al. 2004). IMP proteins are known as oncofetal proteins, reflecting their predominant expression in eggs and embryos, absence in most adult tissues and overexpression in certain carcinomas (Hammer et al. 2005; Dimitriadis et al. 2007; Kobel et al. 2007; for review, see Yisraeli 2005). These proteins play important roles in RNA localization (for review, see Colegrove-Otero et al. 2005; Shav-Tal and Singer 2005; St Johnston 2005), RNA stability (Noubissi et al. 2006; Stohr et al. 2006), translational control (Nielsen et al. 1999; Huttelmaier et al. 2005) as well as cell motility, cell adhesion and invadopodia formation (Yaniv et al. 2003; Vikesaa et al. 2006).

Probably the best understood role of the IMP proteins is in RNA localization, initially described for chicken ZBP1 (IMP1), which promotes translocation of β-actin transcripts to the leading edge of migrating fibroblasts (Ross et al. 1997; Farina et al. 2003) and to growth cone processes in stimulated cultures of embryonic forebrain (Zhang et al. 2001), by interacting with a short zipcode 3′UTR element. Similarly, in *Xenopus* growth cones, Vg1RBP helps target β-actin mRNA asymmetrically in response to attractive growth cues (Leung et al. 2006; Yao et al. 2006). Moreover, *Drosophila* IMP is part of a large motile RNA-containing complex enriched in neurons and in developing oocytes (Barbee et al. 2006; Geng and Macdonald 2006; Munro et al. 2006; Boylan et al. 2008).

In *Xenopus* oocytes, a well-characterized mRNA which undergoes localization to the vegetal cortex during oogenesis is Vg1 mRNA, encoding a member of the transforming growth factor β family implicated in mesoderm formation and the establishment of left–right asymmetry in the developing embryo (King et al. 2005). A portion of the Vg1 mRNA 3′UTR, the vegetal localization element (VLE), promotes localization of reporter RNA in oocytes, in concert with several *trans*-acting factors including Vg1RBP (Deshler et al. 1997; Havin et al. 1998), hnRNP I/PTB (Cote et al. 1999), Prrp (Zhao et al. 2001), and 40LoVe (Czaplinski et al. 2005), in a process that requires microtubules and microfilaments for translocation and anchoring, respectively (Yisraeli et al. 1990). Vg1RBP colocalizes with target mRNAs including Vg1 and VegT mRNA, and Vg1RBP antibodies, injected into oocytes, reduce the amount of correctly localized mRNA (Deshler et al. 1997; Havin et al. 1998; Kwon et al. 2002). Additional components of the Vg1RNP complex, implicated in mediating mRNA localization in oocytes, include Staufen proteins, kinesins and Vg1RBP71/KSRP (Kroll et al. 2002; Allison et al. 2004; Betley et al. 2004; Yoon and Mowry 2004). Considerable insight into the mechanism of the Vg1RNP localization complex assembly has been provided by recent investigations which show that Vg1RBP interacts only indirectly with Vg1 mRNA in the nucleus and that during later stages of the localization pathway the Vg1RNP complex is remodeled by hnRNP I/PTB such that Vg1RBP binds its target RNA directly (Kress et al. 2004; Lewis et al. 2008).

We have undertaken a study of Vg1RNP as oocytes mature meiotically into eggs, when Vg1 mRNA is released from the vegetal cortex. Previous in situ hybridization and biochemical fractionation studies have shown that Vg1 mRNA is no longer tightly associated with the cortex in eggs, although it remains in the vegetal hemisphere (Weeks and Melton 1987; Pondel and King 1988; Forristall et al. 1995). Meiotic maturation of *Xenopus* oocytes, arrested in prophase of meiosis I, is triggered by progesterone, and is manifested by the appearance of a white spot on the pigmented animal hemisphere as the nuclear envelope breaksdown (germinal vesicle breakdown [GVBD]). The process is thought to be initiated via progesterone receptors, which engage several signaling pathways leading to the activation of the phosphatase Cdc25 and the inhibition of the kinase Myt1. This, in turn, results in dephosphorylation and activation of Cdc2/cyclin B (maturation promoting factor, MPF), which plays a key role in the meiotic progression of oocytes. One of the best-characterized pathways triggered by progesterone in *Xenopus* oocytes involves de novo synthesis of the protein kinase Mos, a MAPKKK that activates the Erk2 MAPK cascade. Some effects of Erk2 MAPK in oocytes are mediated by its downstream target p90Rsk, for example, the generation of the ''cytostatic factor'' activity which causes metaphase arrest at the end of meiosis II (Gross et al. 2000, 2001). We report that Vg1RBP is a direct target of Erk2 MAPK during meiotic maturation. We also demonstrate that phosphorylation of Vg1RBP correlates with the release of Vg1 mRNA from the vegetal cortex of the oocyte.

RESULTS

Vg1RBP is redistributed upon meiotic maturation

In oocytes, Vg1RBP has previously been shown to colocalize with Vg1 mRNA at the vegetal cortex (Havin et al. 1998), to cofractionate with the endoplasmic reticulum (ER) after centrifugation of undiluted lysates (Deshler et al. 1997), and to colocalize with vegetal subcortical ER patches (Chang et al. 2004). Similarly, *Xenopus* Staufen1 was reported to be concentrated in the vegetal cortical region, in association with the ER (Allison et al. 2004; Yoon and Mowry 2004). The localization of Vg1RBP and XStau1 was compared, in relation to the ER, in oocytes and progesterone-matured eggs by immunofluorescence.

In oocytes, Vg1RBP is detected in large subcortical patches that colocalize extensively with the ER, in agreement with previous reports (Fig. 1A,A′,A″; Chang et al. 2004). During maturation, as the ER reorganizes to form distinctive, brightly stained whorls (Terasaki et al. 2001), the subcortical Vg1RBP patches are lost as Vg1RBP is released from its cortical anchoring. The remaining Vg1RBP shows very weak, diffuse cytoplasmic staining that does not colocalize with the cortical ER (Fig. 1B,B′,B″). In contrast, the large patches of XStau1 in the vegetal subcortical region of stage VI oocytes remain detectable in eggs (Fig. 1C,D). These observations suggest that Vg1RBP in eggs is released from the cortex, mirroring the fate of Vg1 mRNA, while XStau1 remains in the vegetal subcortical region.

Vg1RBP is phosphorylated upon meiotic maturation

Using Western blotting, we monitored potential modification of Vg1RBP and additional RNA-binding proteins of interest, in stage VI oocytes and progesterone-matured eggs. The migration of Vg1RBP on SDS-PAGE is retarded
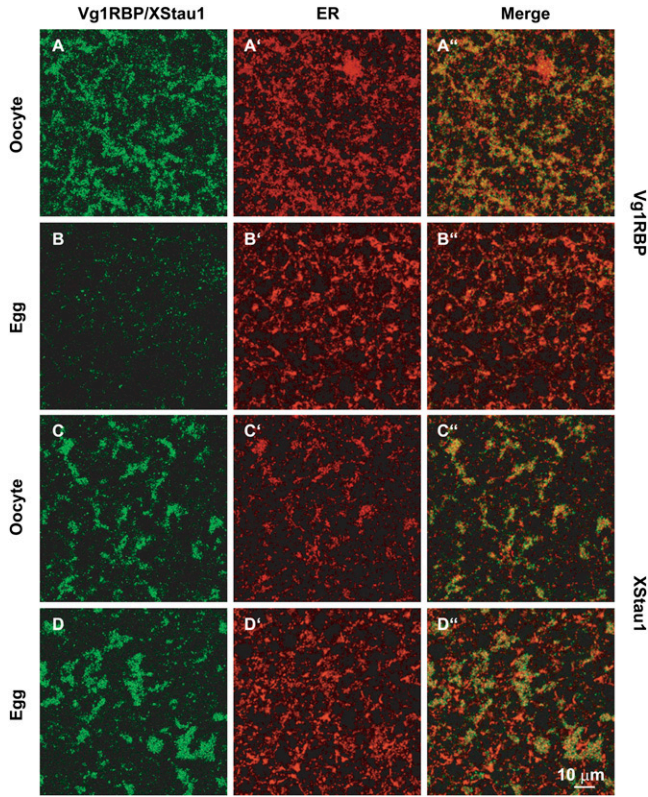
FIGURE 1. Vg1RBP distribution in the vegetal subcortical region of oocytes and eggs. Confocal images of stage VI oocytes and progesterone-matured eggs stained with anti-Vg1RBP (*A,B*) and anti-XStau1 (*C,D*) antibodies. All samples were costained with anti-GRP94 antibodies to visualize the ER (*A′–D′*). (*A″–D″*) are the corresponding overlays of Vg1RBP/XStau1 (green) and GRP94 (red). The confocal sections were taken about 5 μm *below* the vegetal surface in a layer containing distinctive patches containing Vg1RBP and XStau1. Scale bar 10 μm.

in eggs, while the migration of two other VLE-binding proteins, hnRNPI/PTB (Cote et al. 1999) and Prrp (Zhao et al. 2001), was unaffected by maturation (Fig. 2A). XStau1 also undergoes a mobility shift during maturation, as previously noted (Fig. 2A; Allison et al. 2004). Using oocytes and eggs cultured in the presence of ^{33}P-orthophosphate, labeled Vg1RBP was immunoprecipitated from egg, but not oocyte samples, indicating that the shifted forms of the protein incorporated labeled phosphate (Fig. 2B). Last, treatment of the egg samples with the Ser/Thr λ-phosphatase prior to Western blotting reverted the migration of Vg1RBP to that of the oocyte form, showing that it was due to phosphorylated Ser/Thr residue(s) (Fig. 2C).

We then examined the timing of Vg1RBP phosphorylation during meiotic maturation. Figure 3A follows the phosphorylation status of Vg1RBP and the main MAPK pathway components in samples withdrawn at different times from a large population treated with progesterone. Shortly after progesterone addition, cdc2 is dephosphorylated, accompanied by activation of Erk2 MAPK and its

effector p90^{Rsk}, responsible for MII arrest. Surprisingly, Vg1RBP only reaches a fully phosphorylated form after an overnight incubation, placing it as one of the latest reported events in meiotic maturation. Phosphorylation appears to initiate around the time 60% of cells undergo GVBD, but still only about 40% of Vg1RBP is phosphorylated in a sample in which all oocytes have undergone nuclear breakdown (Fig. 3A). To overcome the complications arising from analyzing mixed cell populations, maturation was induced in a large oocyte population and cells that underwent GVBD within a 30-min window were separated (Fig. 3B). Yet again, in these synchronized cells, Vg1RBP phosphorylation reached completion only 12 h after GVBD, while the changes in the phosphorylation status of Erk2 and p90^{Rsk} occurred soon after GVBD. Altogether, this data demonstrates that Vg1RBP phosphorylation is initiated around the time of GVBD, but only completed late during meiotic maturation.

Vg1RBP phosphorylation correlates with release of Vg1 mRNA into the soluble fraction

To examine the biochemical distribution of Vg1 mRNA in maturing oocytes we took advantage of a fractionation method that has been successfully used for surrogate
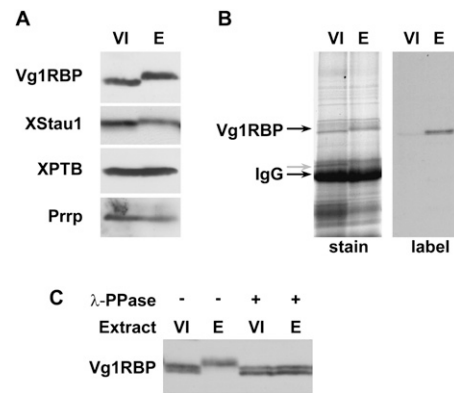

FIGURE 2. Vg1RBP is phosphorylated during meiotic maturation. (*A*) Vg1RBP undergoes an apparent shift in mobility during meiotic maturation. Protein samples from stage VI oocytes (VI) or progesterone-matured eggs (E) were analyzed by Western blotting using antisera directed against the proteins indicated on the *left*. (*B*) Vg1RBP is phosphorylated during meiotic maturation. Stage VI oocytes were incubated overnight in the presence (E) or absence (VI) of progesterone in a medium containing ^{33}P orthophosphate. Vg1RBP was immunoprecipitated using anti-Vg1RBP antiserum and visualized either by autoradiography (*right*) or Coomassie Blue staining (*left*). Note that the overall immunoprecipitation efficiency is similar in both samples. The migration of Vg1RBP and of the IgG heavy chain is indicated. (*C*) The modification of Vg1RBP is phosphatase-sensitive. Protein samples from stage VI oocytes (VI) or progesterone-matured eggs (E) were treated with λ-phosphatase (λ-ppase) and compared to untreated samples using Western blot analysis. Note that under the PAGE conditions employed for this experiment, unmodified Vg1RBP migrates as doublet, reflecting the two allelic variants, A and D.
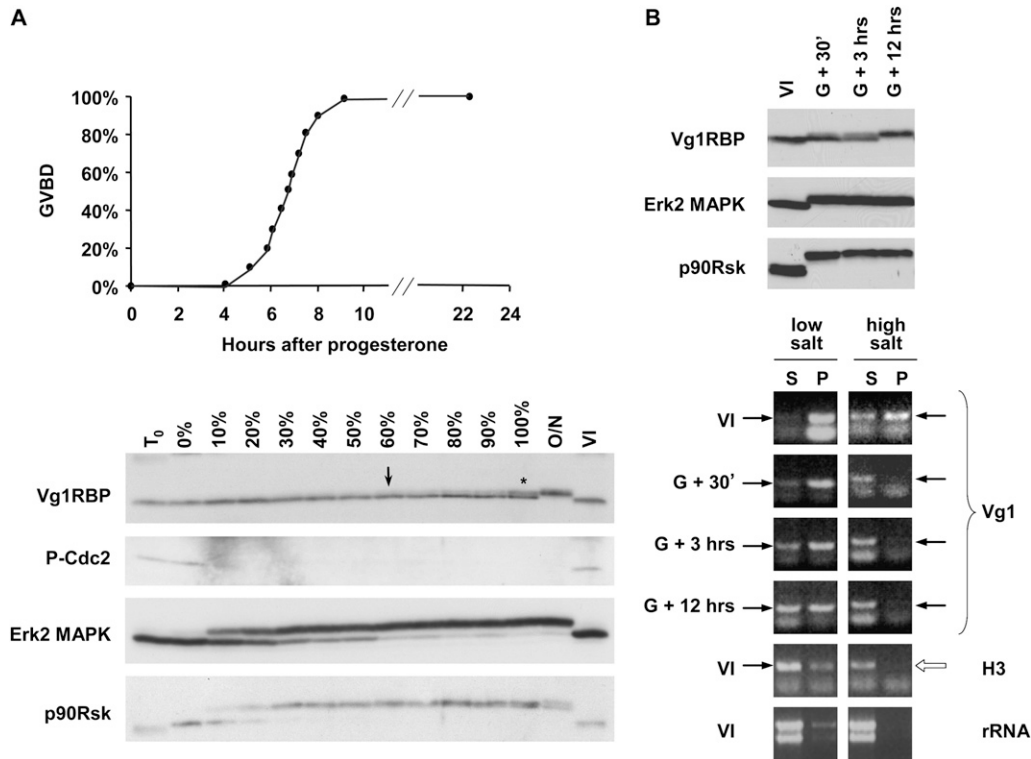
FIGURE 3. Vg1RBP phosphorylation is a late event in meiotic maturation and correlates with release of Vg1 mRNA into the soluble fraction. (*A*) Full phosphorylation of Vg1RBP is a late event in meiotic maturation. Random groups of 10 cells out of ~150 stage VI oocytes treated with progesterone were taken at the time of progesterone addition (T0), when the first GVBD was observed (0%), when the indicated proportion of cells has undergone GVBD (10%–100%) and after an overnight incubation with progesterone (O/N). Control oocytes were incubated for the duration of the experiment in the absence of progesterone (VI). Oocytes were then subjected to Western blot analysis using antisera directed against the proteins indicated on the *left*. Asterisk: ~40% phosphorylation; arrow: earliest visible phospho-Vg1RBP. (*B*) Phosphorylation of Vg1RBP coincides with solubilization of Vg1 mRNA in low-salt conditions. Groups of synchronized stage VI oocytes undergoing maturation were harvested 30 min (G + 30′), 3 h (G + 3 h), or 12 h (G + 12 h) after synchronization. Control oocytes were incubated for the duration of the experiment in the absence of progesterone (VI). Oocytes were then either subjected to Western blot analysis using antisera directed against the indicated proteins (*top* panel) or fractionated into soluble (S) and insoluble (P) fractions in different buffers (see Experimental Procedures for more details). Equivalent proportions of RNA extracted from these fractions was then assayed for the presence of Vg1 and histone H3 mRNAs using nonsaturated RT-PCR. Arrows indicate the diagnostic PCR product. The yield and integrity of extracted RNA was examined by electrophoresis in the presence of ethidium bromide (rRNA).

assessment of cytoskeletal association of vegetal RNAs (Pondel and King 1988; Forristall et al. 1995). Oocytes were extracted in a high salt detergent buffer and the RNA isolated from both the pellet (DIF) and the soluble fraction (DSF). The presence of Vg1 mRNA and control histone H3 mRNA in these fractions was determined by semiquantitative RT-PCR (Fig. 3B). Similarly to the original reports, we observed that Vg1 mRNA shifts from the detergent insoluble (high salt, P) to the soluble fraction (high salt, S) soon after GVBD, representing the breakdown of the cytoskeleton (Becker and Gard 2006). In contrast, the solubilization of Vg1 mRNA in a low-salt detergent-free buffer is a gradual and slow process, which may reflect changes in its mRNP composition or ER association. Consistent with attributing low-salt solubility to noncytoskeletal components, treatment with microtubule or microfilament depolymerizing drugs failed to solubilize Vg1 mRNA under low-salt conditions (data not shown), suggesting that additional

biochemical events take place to that end, possibly involving the ER, cytokeratins, or mRNP components. Importantly, we observed no differences in the yield or integrity of the RNA recovered from different samples estimated by rRNA ethidium bromide staining and histone H3 RT-PCR (Fig. 3B; data not shown). Unfortunately, the high yolk content of stage VI oocytes renders Western blot analysis of low-salt protein pellets or high-salt protein supernatants technically very difficult, thus preventing the evaluation of Vg1RBP solubility in the same samples.

Vg1RBP phosphorylation depends on the MAP kinase pathway

Next, a variety of inhibitors was used to examine the role of the MAPK pathway in Vg1RBP phosphorylation. Blocking Mos/MAPKKK synthesis by injection of anti-*mos* but not control (M3) morpholino oligonucleotides (Dupre et al.

2002) abolished Vg1RBP phosphorylation after an overnight incubation with progesterone (Fig. 4A). This response was dose dependent, since Vg1RBP was partially phosphorylated in samples where Erk2 MAPK was partially active, as evident from its own phosphorylation, but also from the partial phosphorylation of its substrate p90[Rsk] (Fig. 4A, lane E′). Similarly, application of the specific Mek1/MAPKK inhibitor U0126 (Gross et al. 2000), but not the GSK3β inhibitor LiCl (Davies et al. 2000; Bain et al. 2003), resulted in a dose-dependent inhibition of Vg1RBP phosphorylation (Fig. 4B). Importantly, neither of the treatments abolished cdc2 dephosphorylation, suggesting that early meiotic maturation progressed normally. Last, we examined Vg1RBP's phosphorylation status after fertilization, when MAPK is rapidly deactivated (Sohaskey and Ferrell 1999) to allow progression of cell cycle and zygote cleavage, and during embryogenesis up to stage 22/23 embryo. In agreement with the previous results, Vg1RBP phosphorylation mimics that of Erk2 MAPK and p90[Rsk] throughout all stages (Fig. 4C).

Having established the dependence of Vg1RBP phosphorylation on the MAPK pathway, we were prompted by the lateness of the event to locate it downstream from p90[Rsk]. Surprisingly, Ro318220, a potent inhibitor of p90[Rsk], failed to inhibit Vg1RBP phosphorylation (Fig. 4B). Similarly, a >10-fold overexpression of a constitutively active p90[Rsk] (Gross et al. 2001) in stage VI oocytes failed to cause Vg1RBP phosphorylation (data not shown). Failure of both approaches to affect Vg1RBP suggested that its phosphorylation occurred downstream from Mek1/MAPKK but independently of p90[Rsk]. Since constitutively active p90Rsk is well documented to rescue maturation in the absence of MAPK pathway activity (Gross et al. 2001), alternative pathways were considered unlikely. We therefore postulate that although full phosphorylation of Vg1RBP requires an overnight incubation, the extended period for complete Vg1RBP phosphorylation may reflect its high expression levels (see Discussion) since phospho-Vg1RBP is first visible much earlier (Fig. 3A, arrow).
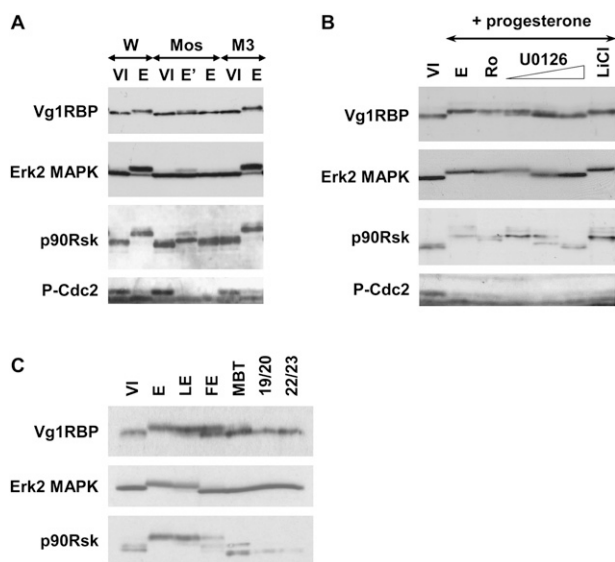
Vg1RBP is phosphorylated on S402

We then proceeded to identify the phosphorylated residue(s) of Vg1RBP. Since yields of immunoprecipitated Vg1RBP were too low for phospho-peptide mapping we recapitulated Vg1RBP phosphorylation in vitro. Following the procedure outlined by Palmer et al. (1998) we showed that extracts derived from eggs, but not oocytes, can drive incorporation of radiolabeled ATP into recombinant His-tagged Vg1RBP in vitro (Fig. 5B, R-K12-K34). Using a series of recombinant His-tagged Vg1RBP truncation variants (summarized in Fig. 5A), we assigned the phosphorylation event to the linker separating the two KH didomains K12 and K34. This inter-KH linker was substrate to phosphorylation by egg, but not oocyte extract regardless of its position within the recombinant protein (Fig. 5A, C-terminal in R-K12-, middle in K12-K34, N-terminal in -K34), or RNA-binding ability (Fig. 5A, cf. -K** and -K34), suggesting that residues 381–414 of Vg1RBP span all the sequences required for its recognition/docking by the kinase as well as the phosphorylation site itself. This is not entirely surprising, since of the 34 residues of this region, 12 are S/T/Y. To aid in identifying potential phosphorylation sites in this region, we analyzed the linker sequence on NetPhos (Blom et al. 1999). Of the 12 S/T/Y residues, S402 had the highest score (0.977). We therefore tested the effect of a point mutation S402 → A (as well as S402 → D) and a control mutation S397 → G on Vg1RBP phosphorylation by egg extracts, and as predicted, mutation of S402 completely abolished phosphorylation of Vg1RBP in vitro (Fig. 5B). To confirm that this phosphorylation site was also utilized in vivo, we followed the phosphorylation of recombinant Vg1RBP variants injected into stage VI oocytes (Fig. 5C). In every set, two proteins were coinjected, of which only one was substrate for in vitro

FIGURE 4. Vg1RBP phosphorylation is dependent on the MAPK pathway. (*A*) Inhibition of Mos synthesis prevents Vg1RBP phosphorylation. Stage VI oocytes were injected with 50 nL of water (W), 0.5 mM anti-Mos morpholino antisense (Mos), or 0.5 mM control morpholino oligonucleotide (M3), and incubated overnight in the presence (E, E′; duplicate samples) or absence (VI) of progesterone. Cells were then subjected to Western blot analysis using antisera directed against the proteins indicated on the *left*. (*B*) Inhibition of Mek1, but not p90Rsk or GSK3β, prevents phosphorylation of Vg1RBP. Stage VI oocytes were preincubated with 5 μM Ro318220, 10, 20, or 50 μM U0126, 10 mM LiCl, or DMSO at comparable concentrations for 4 h and then left overnight in the presence or absence (VI) of progesterone. Cells were then subjected to Western blot analysis using antisera directed against the proteins indicated on the *left*. (*C*) Vg1RBP phosphorylation in embryogenesis correlates with MAPK activity. Protein equivalents of one-stage VI oocyte (VI), progesterone-matured egg (E), laid egg (LE), fertilized egg (FE), MBT embryo, and stage 19/20 or 22/23 neurulas were subjected to Western blot analysis using antisera against the proteins indicated on the *left*.

phosphorylation, either through a deletion that removed the inter-KH linker (Fig. 5C, cf. R-K12-K34 and R-K12ΔK34, R-K12- and R-K12) or through a point mutation of S402. In accord with the earlier results, only the proteins that could be phosphorylated in vitro underwent a retardation in SDS-PAGE mobility upon maturation.

Erk2 MAPK phosphorylates Vg1RBP S402

Interestingly, S402 is followed by a proline residue and resides within an unstructured part of the protein, two features reminiscent of the consensus phosphorylation site for MAP kinases (Davies et al. 2000; Bain et al. 2003). We therefore examined the ability of recombinant in vitro activated MAP kinases (Erk2, p38α, and p38γ) to phosphorylate Vg1RBP directly in an in vitro kinase assay. We found that all three kinases can phosphorylate Vg1RBP, and that this phosphorylation requires S402, but not S397 (Fig. 6A). Moreover, phosphorylation of Vg1RBP by all three MAP kinases caused a retardation of its SDS-PAGE mobility (p38γ example in the bottom panel), similar to that observed for native Vg1RBP upon meiotic maturation. Similar activity and specificity was observed when using extract made from stage VI oocytes injected with the constitutive activator of p38/MAPK, MKK6-DD (Alonso et al. 2000), suggesting that in vivo either the endogenous MAPK associated with meiotic maturation (Erk2) or the artificially triggered stress-related MAPK p38 can phosphorylate Vg1RBP.

To ensure that Vg1RBP phosphorylation by both egg extract and MKK6-DD activated oocytes is truly due to the MAP kinases themselves and not due to activation of secondary components, we examined the sensitivity of these activities to a set of kinase inhibitors. Recombinant Erk2 and p38 MAP kinases were used as reference points (Fig. 6B). Following the detailed inhibitor studies by Davies et al. (2000) and Bain et al. (2003), we included the p38α/β inhibitor SB203580 and Purvalanol A, which inhibits Erk1/2 and members of the Cdk family. To differentiate the two, we also examined the Cdk inhibitor Roscovitine, which does not inhibit Erk2 MAPK. The potency of roscovitine was verified using histone H1 as a substrate for an in vitro kinase assay using egg extracts (data not shown). In addition to these well-established inhibitors, we included the broad-range inhibitors Quercetin (whose potency was verified looking at the activity of CKII against FRGY2, data not shown) and the ATP analog 6-dimethyl aminopurine (6-DMAP), as well as specific inhibitors of the MAPK pathway U0126 (specific against Mek1/MAPKK) and Ro318220 (inhibiting p[90Rsk], but also S6K1, PKC, and GSK3β). In agreement with published data, p38α was highly sensitive to SB203580, while p38γ was resilient to most examined inhibitors, except a slight susceptibility to 6-DMAP. Erk2 MAPK was inhibited by Purvalanol A, and also showed a previously unreported high sensitivity

to 6-DMAP. The inhibition pattern observed for extracts derived from progesterone matured eggs was very similar to that of recombinant Erk2 MAPK (Fig. 6B), consistent with this MAPK being the predominant species in *Xenopus* oocytes (Palmer and Nebreda 2000). In contrast, extracts from MKK6-DD-activated oocytes showed sensitivity to neither SB203580 nor Purvalanol A and only a slight response to 6-DMAP, consistent with the active MAPK species there being p38γ (Fig. 6B). Indeed, Perdiguero et al. (2003) showed that the γ isoform is the major p38 component in *Xenopus* oocytes. Therefore, we concluded that the major contribution to Vg1RBP phosphorylation in meiotic maturation comes from Erk2 MAPK.

FIGURE 5. (Legend on next page)

Interestingly, injection of MKK6-DD, whose activity was monitored by the appearance of phospho-p38, consistently resulted in a partial phosphorylation of Vg1RBP (estimated 60%–70%) in the absence of cell cycle progression (cdc2 is still phosphorylated while Erk2 MAPK and p90[Rsk] are not; Fig. 6C). This was not affected by preincubation with U0126, eliminating the involvement of a p38–Erk2 cross-talk activation. The reasons why p38 activation never results in full phosphorylation of Vg1RBP are at present unknown, but we speculate that complete Vg1RBP accessibility requires maturation-dependent reorganization of the cortical region.

Inhibition of phosphorylation with U0126 prevents release of Vg1RBP and Vg1 mRNA in eggs, while premature phosphorylation of Vg1RBP by MKK6-DD in oocytes partly releases Vg1RBP from the cortex and solubilizes Vg1 mRNA

We then examined the effect of U0126 and MKK6-DD on the subcellular association of Vg1RBP and Vg1 mRNA. First, we examined the subcortical distribution of Vg1RBP, in relation to the ER, by confocal immunofluorescence (Fig. 7B). In Stage V1 oocytes, Vg1RBP is concentrated in large patches which coincide with dense regions of ER (Fig. 7B, panels A,A′; also see Fig. 1). U0126 treatment blocked the reorganization of these structures which normally occurs during maturation and the dispersion of the Vg1RBP staining. The subcortical ER/Vg1RBP patched remained intact and appeared to spread out and flatten, tending to fuse together in a layer parallel to the egg surface (Fig. 7B, panels C,C′). In MKK6-DD injected eggs, Vg1RBP also remained associated with subcortical ER patches, although these adopted a more dispersed organization similar to that seen in unfertilized eggs (Fig. 7B, panels B,B′) but positioned more deeply (Fig. 7B, panels D,D′).

FIGURE 5. Vg1RBP is phosphorylated on Serine 402. (*A*) Schematic representation of recombinant Vg1RBP variants and their nomenclature. Black: RRMs, dark gray: KH domains, light gray: unstructured sequences, N: point mutations in KH domains which abrogate RNA binding. The wild-type sequence of the inter-KH linker (spanning residues 381–414) is boxed; internal deletions are showed as hyphens, point mutations are in lowercase, the position of serines 397 and 402 is indicated below. The drawing is not to scale. (*B*) Serine 402 is phosphorylated in vitro; 15 pmol of each of the indicated Vg1RBP variants was used as a substrate in an in vitro kinase assay using extracts derived from either stage VI oocytes (VI) or progesterone-matured eggs (E). Samples were visualized using autoradiography (*top* panel) and Coomassie Blue staining (*bottom* panel). (*C*) Serine 402 is phosphorylated in vivo. Pairs of equimolar recombinant Vg1RBP variants were injected into stage VI oocytes, which were then incubated overnight in the presence (E) or absence (VI) of progesterone. Protein extracts from duplicate samples were subjected to Western blot analysis using anti-His antibody alongside samples of the injected mixtures (*input*). Injected proteins are indicated with the larger protein *above* the smaller protein. Note that due to differential stability of the injected proteins, samples from R-K12/R-K12- injected cells represent two rather than one cell equivalents.

The partial dispersion of the Vg1RBP patches in MKK6-DD eggs, compared to progesterone-matured eggs, possibly reflects the partial Vg1RBP phosphorylation obtained in this treatment (Fig. 6C).

As we showed earlier, Vg1 mRNA solubilization can be readily assessed in vitro, using oocyte lysates. We therefore examined the solubility of Vg1 mRNA in similarly treated oocytes. Typically, in low salt buffers, Vg1 mRNA is essentially insoluble in lysates prepared from stage VI oocytes (Fig. 7A, samples 2,5,10), when Vg1 mRNA is enriched at the vegetal cortex in vivo. In contrast, it is soluble in stage II lysates, where Vg1 mRNA is homogeneously distributed in the cytoplasm and its translocation to the cortex is yet to be initiated (Fig. 7A, samples 1,9; King et al. 2005). We examined the effect of Vg1RBP phosphorylation on the solubility of Vg1 mRNA in this assay. Figure 7A shows three independent experiments (grouped by brackets) employing semiquantitative RT-PCR analysis of Vg1 mRNA in soluble and insoluble fractions. Two main observations were made. First, in the presence of U0126 a larger proportion of Vg1 mRNA remains insoluble upon progesterone treatment (Fig. 7A, cf. samples 3 and 4). Second, injection of MKK6-DD, irrespective of U0126, causes an increase in soluble Vg1 mRNA (Fig. 7A, cf. samples 6,7 and 5, samples 11 and 10, samples 13 and 12). Histone H3 mRNA was equally soluble in all treatments (Fig. 7A, an example is shown in sample 14). In summary, the imaging and the fractionation experiments indicate that cell cycle progression in the absence of Vg1RBP phosphorylation (presence of U0126) reduces solubilization of Vg1 mRNA/Vg1RBP while Vg1RBP phosphorylation in the absence of cell cycle progression (MKK6-DD injection) increases Vg1 mRNA/Vg1RBP solubility.

The changes in Vg1 mRNP are not due to changes in either of two activities of Vg1RBP previously investigated in our lab, namely, binding to its cognate RNA target and self-association (Git and Standart 2002). RNA binding was assessed by UV cross-linking (Fig. 8A), where uniformly labeled VLE RNA probe was mixed with a series of recombinant Vg1RBP variants, some of which were pre-phosphorylated by recombinant in vitro activated p38α MAPK. The in vitro phosphorylation was driven to completion as evident from retardation of SDS-PAGE mobility (data not shown). Neither of the full-length variants showed an altered binding to the VLE, be it point mutants abolishing the phosphorylation site (Fig. 8A, S402 → A) or mimicking a phosphorylated site (Fig. 8A, S402 → D). No difference was observed employing preincubation of the full-length wild-type and S397 → G variants with either an active form p38α MAPK (p38α**; Vg1RBP phosphorylation evident as retarded migration of the radiolabeled protein) or its inactive counterpart. In fact, the inter-KH linker can be removed in halves or in its entirety with no detrimental effect on UV cross-linking to the VLE
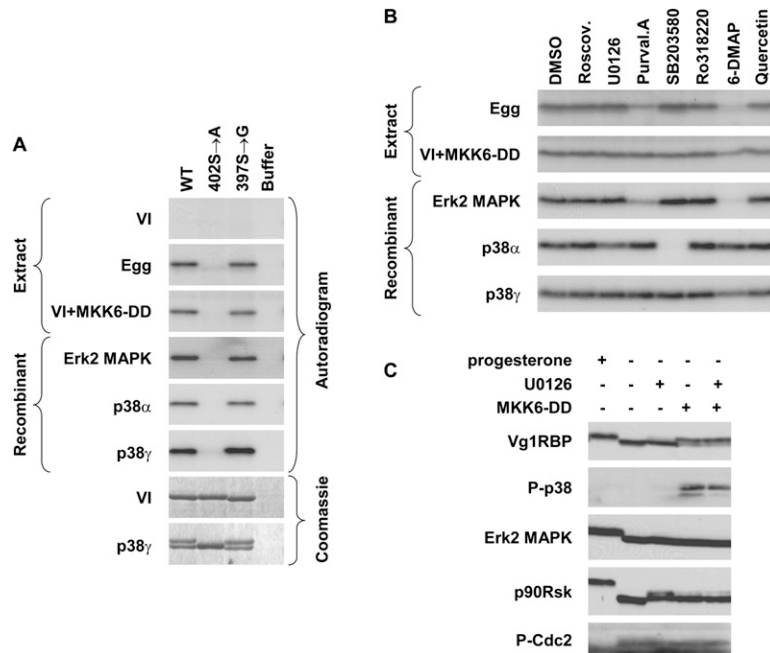
FIGURE 6. Vg1RBP is phosphorylated by MAPK. (A) Serine 402 can be phosphorylated by both Erk2 and p38 MAP kinases; 15 pmol of recombinant full-length wild-type (WT), S402 → A or S397 → G Vg1RBP variants or buffer alone were used as substrates for in vitro kinase assays with 10 ng recombinant in vitro-activated Erk2, p38α, or p38γ or extracts made from stage VI oocytes (VI), progesterone-matured eggs (E), and stage VI oocytes injected with MKK6-DD (VI + MKK6-DD). Samples were visualized using autoradiography and Coomassie Blue staining. (B) The phosphorylation of Vg1RBP by egg extract is sensitive to Erk2 MAPK but not p38/MAPK inhibitors; 15 pmol wild-type recombinant Vg1RBP was used as a substrate for in vitro kinase assays using kinases and extracts as above in the presence of the following inhibitors: 10 μM Roscovitine, 20 μM U0126, 10 μM Purvalanol A, 10 μM SB203580, 1 μM Ro328220, 1 mM 6-DMAP, or 20 μM Quercetin. A similar volume of DMSO was used as a control. (C) In vivo activation of p38 MAPK leads to Vg1RBP phosphorylation in the absence of cell cycle progression. Stage VI oocytes were preincubated for 4 h with 50 μM U0126 or equivalent concentrations of DMSO, microinjected with 50 nL of 1.5 mg/mL MKK6-DD and incubated overnight alongside with progesterone-treated oocytes. Cells were then subjected to Western blot analysis using antisera directed against the proteins indicated on the *left*.

residue is S402, which is located between KH2 and KH3 domains, and that this modification, while not affecting RNA-binding or self-association of Vg1RBP, correlates with the release of Vg1 mRNA from the vegetal cortex in vivo, and in vitro. Previously, we showed that *Xenopus* Staufen 1 is also phosphorylated by MAPK during meiotic maturation, albeit with different kinetics (Allison et al. 2004), although as we show here XStau1 remains in the subcortical region in eggs. In contrast to the early phosphorylation of Staufen proteins, full phosphorylation of Vg1RBP is a very late event in meiotic maturation. We propose that the extended period it takes Vg1RBP to fully phosphorylate may reflect its high levels, ~50–100 ng per oocyte (Git and Standart 2002) and possibly suboptimal phosphorylation site. Consistent with this hypothesis, *Xenopus* Staufen proteins are present in oocytes at 10–20-fold lower levels (Allison et al. 2004).

Interestingly, the linker bridging KH2 and KH3 in IMP1 is a target of *c-src* kinase, which phosphorylates a key tyrosine residue, and in the case of chicken ZBP1 (..AAPY$_{396}$SS..) reduces its binding to β-actin mRNA, resulting in its translational activation at the cell periphery (Huttelmaier et al. 2005). Similarly, *c-src* phosphorylation of the translational repressor hnRNP K, in its KH3 domain, reduces its RNA-binding, promoting translation initiation (Ostareck-Lederer et al. 2002; Messias et al. 2006).

The equivalent tyrosine residue in IMP3 proteins may be Y409 (in *Xenopus*, ..STSY$_{409}$PP..), as, similar to chick IMP1, this tyrosine lies just downstream from a potential SH3-like *c-src* docking domain (Huttelmaier et al. 2005). It is interesting to note that phosphorylation of residues separated by only six amino acids has such different effects on RNA-binding of IMP proteins. Recent studies show that *c-src* kinase is inactive in *Xenopus* eggs, and is only activated upon fertilization (Iwasaki et al. 2008), suggesting that *c-src* kinase, if it phosphorylates IMP3/Vg1RBP in embryos, may modify a protein that has been phosphorylated by MAPK previously. While speculative, such a scenario is plausible as the *c-src* site is apparently conserved between vertebrate IMP1 and IMP3 proteins, including Vg1RBP (see Supplemental Fig. 1). However, regarding the conservation of MAPK sites in this linker region, we note that while potential SP/TP sites are not universally present in all three protein families their prevalence suggests the possibility of
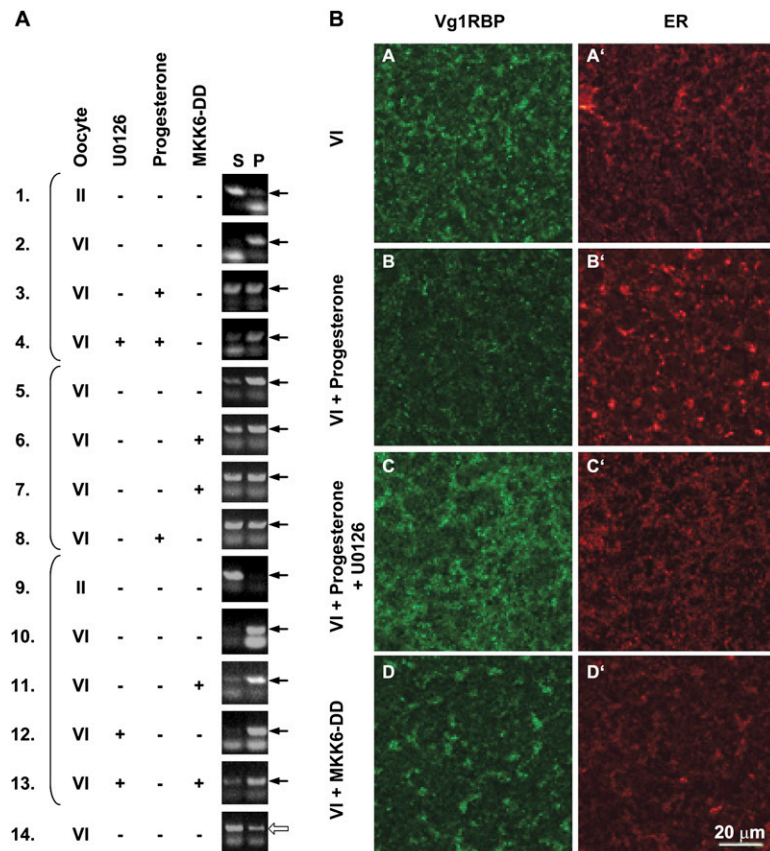
(R-K12ΔK34, R-K12CK34, R-K12NK34). This is in contrast with truncations that remove either of the KH didomains (R-K12- and -K34), previously shown to be required for RNA binding (Git and Standart 2002). Similarly, deletion of the inter-KH linker, mutations of S402 or preincubation of the wild-type full-length with active or inactive p38α MAPK do not affect the ability of Vg1RBP to self-associate, as measured by appearance of a dimer-size protein upon addition of the bivalent cross-linker DMS (Fig. 8B). Therefore, the changes in Vg1RBP affect the biochemical fate of its target mRNA not through direct interactions with the RNA or itself, but probably due to changes in interactions with third-party components, such as other Vg1 mRNP proteins, the cytoskeleton or ER.

DISCUSSION

Our work shows that Vg1RBP is phosphorylated by Erk2 MAPK during meiotic maturation, that the single modified

FIGURE 7. Vg1RBP phosphorylation correlates with its cortical detachment and solubilization of Vg1 mRNA. (*A*) The solubility of Vg1 mRNA in low salt buffer correlates with the phosphorylation of Vg1RBP. Stage VI oocytes were preincubated with 50 μM U0126 where indicated and then either injected with 50 nL 1.5 mg/mL MKK6-DD or exposed to progesterone. Control stage II and VI oocytes were incubated for the duration of the experiment without any treatment. After a 16-h incubation, oocytes were fractionated into soluble (S) and insoluble (P) fractions in low salt buffer. Equivalent proportions of RNA extracted from these fractions was then assayed for the presence of Vg1 (samples 1–13) or histone H3 (sample 14) mRNAs using nonsaturated RT-PCR. Arrows indicate the diagnostic PCR product. Brackets group samples that originated from the same experiment. (*B*) Vg1RBP phosphorylation correlates with its cortical release. Confocal images of stage VI oocytes (VI), oocytes matured by addition of progesterone in the absence or presence of 50 μM U0126 and stage VI oocytes injected with MKK6-DD (VI + MKK6-DD), stained with anti-Vg1RBP (A–D) and anti-GRP94 antibodies (visualizing the ER; A′–D′). Confocal images from equivalent subcortical layers near the vegetal pole are shown, except for the MKK6-injected oocytes where the slightly deeper layer to which the ER-Vg1RBP patches have sunk is shown. Scale bar: 20 μm.

oocytes and in eggs. This has allowed us to propose a model whereby the release of Vg1 mRNA from its tight association with the cortex during meiotic maturation has two components. First, breakdown of cytoskeletal structures shortly after GVBD releases Vg1 mRNA from the detergent insoluble fraction, whereas in low salt conditions it remains in insoluble complexes. Later, correlating with the kinetics of Vg1RBP phosphorylation, Vg1 mRNA is at least partially released from these structures into the soluble fraction (Fig. 9). Clearly, it will be interesting to identify these additional Vg1RBP partners to understand the function of S402 phosphorylation. While the molecular details of the role of Vg1RBP targeting by MAPK remain to be elucidated, identification of the modified residue and the evidence that S402 phosphorylation of Vg1RBP likely impacts on protein–protein or ER interactions, but not RNA-binding or self-association, provide an important contribution to studies of IMP proteins. Interestingly, recent studies in line with our data show that in *Xenopus* oocytes Vg1RNA localization to the vegetal cortex results from RNP remodeling regulated by PTB/hnRNP I. Vg1RNP assembly, initiated in the nucleus, involves indirect binding of Vg1RBP to Vg1 mRNA, via PTB and possibly other RNP proteins. Later, during the localization pathway, the RNP is remodeled, such that Vg1RBP binds Vg1 mRNA directly (Lewis et al. 2008). Rand and Yisraeli (2007) report that Vg1 mRNA localization occurs in the absence of Vg1RBP RNA-binding, and correlates with its association with microtubules, also emphasizing the importance of protein:protein, rather than protein:RNA, interactions for Vg1RBP function. Moreover, as the inter-KH linker was shown to be dispensable for Vg1 RNA localization in oocytes (Rand and Yisraeli 2007), it may play a regulatory role during maturation or later in development.

differential regulation. Within any one species, there are orthologs that contain such sites (usually IMP3) and orthologs devoid of such sites (usually IMP1). We also note that the SP/TP sites in IMP2 proteins often reside in what seem to be alternatively spliced exons (see Supplemental Fig. 1). *Drosophila* IMP (dIMP) also contains potential MAPK TP sites in the KH2/KH3 linker; and preliminary experiments indicate that the mobility of dIMP is altered in embryo relative to ovary samples, consistent with phosphorylation (R. Habedanck, A. Git, and N. Standart, unpubl.).

We adapted a previously described fractionation method to assess the cytoskeletal association of vegetal RNAs in portance of protein:protein, rather than protein:RNA, interactions for Vg1RBP function. Moreover, as the inter-KH linker was shown to be dispensable for Vg1 RNA localization in oocytes (Rand and Yisraeli 2007), it may play a regulatory role during maturation or later in development.

In summary, we provide evidence that Vg1RBP (IMP3) undergoes MAPK-dependent phosphorylation on S402 located between KH2 and KH3 RNA-binding domains during meiotic maturation of *Xenopus* oocytes. While this modification has no effect on the ability of Vg1RBP to bind RNA or for its self-association, it likely impacts on its
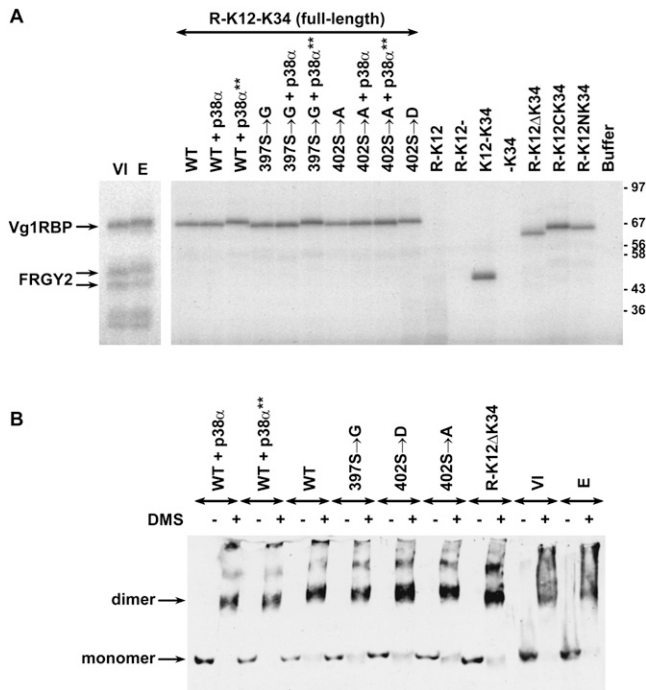
A

B

FIGURE 8. Vg1RBP phosphorylation does not affect its RNA binding or self-association. (*A*) Phosphorylation of Vg1RBP does not affect RNA binding. S10 extracts from stage VI oocytes (VI) or progesterone-matured eggs (E) and 0.75 pmol recombinant Vg1RBP variants were tested in a UV cross-linking assay using VLE RNA probe uniformly labeled with [α-^{32}P]-UTP. Where indicated, proteins were prephosphorylated with recombinant in vitro activated p38α (+ p38α**). A parallel reaction with inactive p38α (+ p38α) was used as a control. The samples were resolved using SDS-PAGE and visualized by autoradiography. (*B*) Phosphorylation of Vg1RBP does not affect self association. S10 extracts from stage VI oocytes (VI) or progesterone-matured eggs (E) and 15 pmol recombinant Vg1RBP variants were cross-linked by addition of 1.5 mg/mL dimethyl suberimidate (DMS) in borate buffer (+) or borate buffer alone (−). Where indicated, proteins were prephosphorylated as above. Samples were resolved on phosphate SDS-PAGE gel and subjected to Western blot analysis using anti-Vg1RBP antiserum. Migration of monomer and dimer forms is indicated on the *left*.

interactions with other proteins of the Vg1 RNP or the cytoskeleton/ER.

MATERIALS AND METHODS

Plasmids and recombinant proteins

Expression constructs encoding wild-type (allele D) full-length Vg1RBP-His, N- and C-terminal deletion mutants (R-, R-K12, K12-K34, -K34, K34) and the C-terminal KH didomain carrying two mutations abolishing RNA binding (-K**, K**) have been described previously (Git and Standart 2002). For simplicity of annotation, the variant previously designated R-K12+ is referred to as R-K12. An additional deletion mutant (R-K12-, spanning residues 1-413 of the Vg1RBP ORF) was cloned similarly using the primers CATG-CCATGG-ACAAGCTGTATATT and CG-CTCGA G-CCCAAATGGTGGATAAG. Deletion of the inter-KH linker

was achieved in two steps. First, a silent mutation creating a unique MscI restriction site was introduced at position 1616 of the cDNA using the primers 5′-CTTATCCACCATTT<u>TGGcCA</u>GCAGC CAGAGTC-3′ and 5′-GACTCTGGCTGCTGgCCAAATGGTGGA TAAG-3′ (MscI site is underlined, mutated nucleotides are in lowercase). The new site was then used to remove an NsiI–MscI fragment spanning the inter-KH linker. Mutagenesis of S397 → G, S402 → A, S402 → D was achieved using the following oligonucleotide pairs (new restriction sites are underlined, mutated nucleotides are in lowercase):

5′-ATCAGGAATGCCACCc<u>CCggg</u>TGTTGGAGTTCCCTC-3′ and
    5′-GAGGGAACTCCAAC<u>Accc</u>G<u>G</u>gGGTGGCATTCCTGAT-3′;
5′-CCTTCTGTTGGAGTTCC<u>ggcg</u>CCTACCTCATCTACTTC-3′
    and 5′-GAAGTAGATGAGGTA<u>GGcgcc</u>GGAACTCCAACAGA
    AGG-3′; and
5′-CCTTCTGTTGGAGTTCC<u>ggat</u>CCTACCTCATCTACTTC-3′
    5′-GAAGTAGATGAGGTA<u>GGatcc</u>GGAACTCCAACAGAAGG.

The SmaI site co-introduced with the S397 → G was also used to remove NsiI-SmaI or SmaI-MscI fragments spanning the N- and C-terminal halves of the inter-KH linker, respectively. All mutagenesis was performed using the Quickchange protocol (Stratagene) and all constructs were verified by sequencing.

Overexpression and purification of recombinant proteins was carried out as described in Git and Standart (2002). All Vg1RBP variants used in this study expressed to similar levels and had similar solubility and purification profiles. Recombinant kinases (MalE-MKK6-DD, MalE-Xp38α, and in vitro activated MalE-XMpk1/Erk2 and GST-Xp38γ (Git and Standart 2002), referred to as recombinant MKK6-DD, p38α, Erk2, and p38γ, respectively, were prepared as described previously (Perdiguero et al. 2003).

Antibodies

Rabbit polyclonal antibodies against full-length Vg1RBP and XStau1 have been described in Allison et al. (2004). Rabbit polyclonal antisera against *Xenopus* VgRBP60/hnRNP-I and Prrp were gifts from K. Mowry and P. Huber, respectively. Antiphospho-cdc2 and antiphospho-p38 antibodies were from Cell Signaling (#9111 and #9211), anti-Erk1/2 and anti-p90^{Rsk1} antibodies were from Santa Cruz Biotechnology (sc-94 and sc-231-g), anti-His antibody was from Qiagen (34660), and anti-GRP94 from StressGen Biotechnologies. All secondary antibodies for Western blot analysis were horseradish peroxidase conjugates, and FITC/rhodamine conjugates for confocal imaging (Jackson Immunoresearch).

Western blot analysis

Dry frozen oocytes, eggs, or dejellied laid eggs and embryos were lysed in cold BFH (20 mM Tris at pH 7.4, 50 mM NaCl, 12.5 mM β-glycerophosphate, 15 mM NaF, 10 mM EGTA, 2 mM MgCl$_2$, 6 mM DTT, 1× Roche Complete EDTA-free Protease Inhibitors) to a final 5–20 μL/cell. The extract was cleared from yolk and debris for 10 min at 14,000 rpm and the supernatant denatured in protein sample buffer; 0.75–2 cell equivalents were resolved on SDS-PAGE and electrotransferred onto an Immobilon-P membrane (Millipore). The membrane was then blocked and probed following standard protocols using TBST (150 mM NaCl, 50 mM Tris-HCl at pH 7.5, 0.1% Tween-20) supplemented at the blocking and probing stages with either 4.5% BSA (for
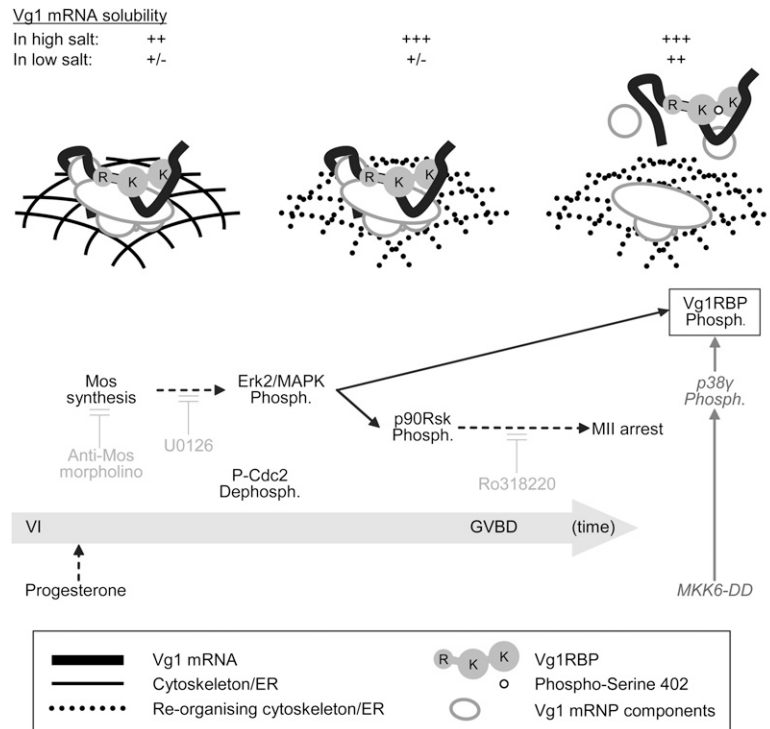
FIGURE 9. A two-step model for the release of Vg1 mRNA from the cortex in meiotic maturation. Initiating triggers for the phosphorylation of Vg1RBP (boxed) are indicated at the *bottom* (application of progesterone or microinjection of MKK6-DD) with the physiological pathway arranged temporally (from *left* to *right*; not to scale). The components contributing to Vg1 mRNA's subcortical anchoring at the key stages are represented in the main illustration (see key in the figure). The solubility of Vg1 mRNA in high or low salt buffers is indicated above. The activity of several inhibitors used throughout this study is in light gray. Direct links are in solid arrows and indirect connections are in dashed arrows. Phosph., phosphorylation; R, RRMs; K, KH didomains.

antiphospho-p38) or 2% skim milk powder (Marvel; for all other antibodies). Antibodies were visualized using enhanced chemiluminescence.

For phosphatase assays, dry frozen oocytes or eggs were lysed in $1\times$ λ-phosphatase buffer supplemented with $1\times$ Roche Complete EDTA-free Protease Inhibitors and cleared for 10 min at 14 000 rpm. λ-Phosphatase (250 ng) (New England Biolabs P0753S) and 2 mM $MnCl_2$ were added according to manufacturer's recommendations. Following a 1-h incubation at 30°C samples were subjected to Western blot analysis.

Oocyte handling, maturation, and microinjection

Stage VI oocytes were manually sorted from a collagenase-treated ovary and incubated in MBS (88 mM NaCl, 1 mM KCl, 0.41 mM $CaCl_2$, 0.33 mM $Ca(NO_3)_2$, 0.82 mM $MgSO_4$, 2.4 mM $NaHCO_3$, 10 mM HEPES at pH 7.4). Meiotic maturation was induced by addition of 10 µg/mL progesterone (Sigma P-0130) for 16 h. Synchronous samples were obtained by inducing maturation in a large oocyte population and separating cells that underwent GVBD within a 30-min window. Where indicated, oocytes were preincubated with U0126 (Promega #V1121), Ro318220 (Calbiochem 557520), or LiCl for 4 h prior to addition of progesterone. All inhibitors were added at concentrations suggested by Davies

et al. (2000) and Bain et al. (2003), except U0126 that was used at 20–50 µM instead of 10 µM.

Microinjection of recombinant Vg1RBP variants, MalE-MKK6DD and αMos morpholino oligonucleotides was performed using the following equipment: MZ6 stereoscopic light microscope (Leica), PLI-100 microinjector (Medical Systems Corp.) and MM-3 micromanipulator (Narishige). Needles were made by pulling GD-1 capillaries on a PB-7 needle puller (Narishige). All injected samples were in 30–50 nL.

Confocal imaging of *Xenopus* oocytes was previously described (Allison et al. 2004).

In vivo labeling and immunoprecipitation

Stage VI oocytes were incubated in MBS containing 0.5 mCi/mL phosphorus-33 (Amersham Biosciences BF1003). After 6 h, progesterone was added to half the samples and the cells were left for 16 h to complete maturation. [33]P uptake from the buffer was measured by scintillation counting and ranged between 60% and 80%. Within each experiment, no differences were observed between oocyte and egg samples.

Thirty oocytes were lysed in BFH to a final 2 µL/cell, cleared for 10 min in a minifuge, and diluted 10-fold in NET+ (50 mM Tris-HCl at pH 7.5, 500 mM NaCl, 0.5% NP-40, 1 mM EDTA, 0.25% gelatin, 0.02% sodium azide, 20 mM NaF) supplemented with 2% BSA. The lysate was then mixed with either preimmune or anti-Vg1RBP antiserum prebound to protein A-Sepharose (Amersham Biosciences 17-0963-03) for 2 h at 4°C and washed extensively in NET+. The immunoprecipitated proteins were eluted in protein sample buffer, resolved on SDS-PAGE, and visualized by autoradiography.

In vitro kinase assay

Ten microliter reactions were set up in H1K buffer (80 mM β-Glycerophosphate, 20 mM EGTA, 15 mM $MgCl_2$, 1 mM DTT, $1\times$ Roche Complete EDTA-free protease inhibitors, 50 µM ATP) supplemented with 0.5–2 µCi [γ-^{32}P]-ATP. The reactions contained 10 ng recombinant kinase or 0.1 oocyte equivalent of extract, kinase inhibitors where indicated and 15 pmol of substrate (1 µg full-length Vg1RBP variants and equimolar amounts of smaller variants). Samples were incubated at room temperature for 30 min prior to SDS-PAGE electrophoresis, Coomassie Blue staining, and autoradiography. Where appropriate, control reactions were performed using commercially available substrates, such as Histone H1 or Myelin Basic Protein (data not shown). Roscovitine, SB203580 and Purvalanol A were from Calbiochem (557360, 559398, and 540500, respectively), Quercetine and 6-dimethylaminopurine (6-DMAP) were from Sigma (Q-0125 and D-2629, respectively).

UV cross-linking and DMS cross-linking

Recombinant full-length Vg1RBP variants (2.5 μg) were in vitro phosphorylated by incubation with 400 ng in vitro activated MelE-Xp38α in H1K buffer for 1 h at room temperature. Control samples were incubated with inactive MelE-Xp38α or buffer alone. Protein phosphorylation was assessed by Coomassie Blue staining of SDS-PAGE gels to approach 100%.

UV cross-linking and dimethyl-suberimidate (DMS) cross-linking were described in Git and Standart (2002). BSA and nonself-associating variants of Vg1RBP were included as negative controls in the DMS experiments (data not shown).

RNA fractionation and RT-PCR

Dry frozen oocytes were resuspended in either BFH or HSDB (1% Triton X100, 0.5 M KCl, 10 mM Pipes at pH 6.8, 5 mM MgOAc, 1 mM EGTA, 300 mM sucrose, 0.2 mg/mL heparin, 12.5 mM β-glycerophosphate, 15 mM NaF, 1× Roche Complete EDTA-free Protease Inhibitors) to a final 10 μL/cell. The resulting lysates were incubated on ice for 30 min and spun for 10 min at 14 krpm. Following removal of the clear supernatants, pellets were resuspended in BFH. Proteins were digested in PK solution (100 mM Tris at pH 7.5, 300 mM NaCl, 5 mM EDTA, 2% SDS, 200 μg/mL Proteinase K, 12.5 ng/μL calf liver tRNA) for 1–2 h at 50°C and RNA was extracted by 1:1 phenol:chloroform followed by chloroform alone and finally ethanol precipitated. BFH and HSDB samples taken through the purification procedure were used as negative controls. Recovery and integrity of rRNA was monitored by agarose gel electrophoresis.

RNA equivalent to 0.25 oocyte was reverse transcribed using AMV-RT (Promega) primed with random hexamers according to manufacturer's instructions. 1/20th of the resulting cDNA was used as a template for PCR using the following primers (histone H3 3280 and 3281, VTE Vg1 primers Q9252/53 or OL 140/141) for 28 cycles of 95°C, 40°C, 72°C steps each for 30 sec. Neither the RT nor the PCR steps were under saturating conditions.

SUPPLEMENTAL MATERIAL

Supplemental material can be found at http://www.rnajournal.org.

REFERENCES

Allison, R., Czaplinski, K., Git, A., Adegbenro, E., Stennard, F., Houliston, E., and Standart, N. 2004. Two distinct Staufen isoforms in *Xenopus* are vegetally localized during oogenesis. *RNA* **10:** 1751–1763.

Alonso, G., Ambrosino, C., Jones, M., and Nebreda, A.R. 2000. Differential activation of p38 mitogen-activated protein kinase isoforms depending on signal strength. *J. Biol. Chem.* **275:** 40641–40648.

Bain, J., McLauchlan, H., Elliott, M., and Cohen, P. 2003. The specificities of protein kinase inhibitors: An update. *Biochem. J.* **371:** 199–204.

Barbee, S.A., Estes, P.S., Cziko, A.M., Hillebrand, J., Luedeman, R.A., Coller, J.M., Johnson, N., Howlett, I.C., Geng, C., Ueda, R., et al. 2006. Staufen- and FMRP-containing neuronal RNPs are structurally and functionally related to somatic P bodies. *Neuron* **52:** 997–1009.

Becker, B.E. and Gard, D.L. 2006. Visualization of the cytoskeleton in *Xenopus* oocytes and eggs by confocal immunofluorescence microscopy. *Methods Mol. Biol.* **322:** 69–86.

Betley, J.N., Heinrich, B., Vernos, I., Sardet, C., Prodon, F., and Deshler, J.O. 2004. Kinesin II mediates Vg1 mRNA transport in *Xenopus* oocytes. *Curr. Biol.* **14:** 219–224.

Blom, N., Gammeltoft, S., and Brunak, S. 1999. Sequence- and structure-based prediction of eukaryotic protein phosphorylation sites. *J. Mol. Biol.* **294:** 1351–1362.

Boylan, K.L., Mische, S., Li, M., Marques, G., Morin, X., Chia, W., and Hays, T.S. 2008. Motility screen identifies *Drosophila* IGF-II mRNA-binding protein–zipcode-binding protein acting in oogenesis and synaptogenesis. *PLoS Genet.* **4:** e36. doi: 10.1371/journal.pgen.0040036.

Chang, P., Torres, J., Lewis, R., Mowry, K., Houliston, E., and King, M.L. 2004. Localization of RNAs to the mitochondrial cloud in *Xenopus* oocytes by entrapment and association with endoplasmic reticulum. *Mol. Biol. Cell* **15:** 4669–4681.

Colegrove-Otero, L.J., Minshall, N., and Standart, N. 2005. RNA-binding proteins in early development. *Crit. Rev. Biochem. Mol. Biol.* **40:** 21–73.

Cote, C.A., Gautreau, D., Denegre, J.M., Kress, T.L., Terry, N.A., and Mowry, K.L. 1999. A *Xenopus* protein related to hnRNP I has a role in cytoplasmic RNA localization. *Mol. Cell* **4:** 431–437.

Czaplinski, K., Kocher, T., Schelder, M., Segref, A., Wilm, M., and Mattaj, I.W. 2005. Identification of 40LoVe, a *Xenopus* hnRNP D family protein involved in localizing a TGF-β-related mRNA during oogenesis. *Dev. Cell* **8:** 505–515.

Davies, S.P., Reddy, H., Caivano, M., and Cohen, P. 2000. Specificity and mechanism of action of some commonly used protein kinase inhibitors. *Biochem. J.* **351:** 95–105.

Deshler, J.O., Highett, M.I., and Schnapp, B.J. 1997. Localisation of *Xenopus* Vg1 mRNA by Vera protein and the endoplasmic reticulum. *Science* **276:** 1128–1131.

Dimitriadis, E., Trangas, T., Milatos, S., Foukas, P.G., Gioulbasanis, I., Courtis, N., Nielsen, F.C., Pandis, N., Dafni, U., Bardi, G., et al. 2007. Expression of oncofetal RNA-binding protein CRD-BP/IMP1 predicts clinical outcome in colon cancer. *Int. J. Cancer* **121:** 486–494.

Dupre, A., Jessus, C., Ozon, R., and Haccard, O. 2002. Mos is not required for the initiation of meiotic maturation in *Xenopus* oocytes. *EMBO J.* **21:** 4026–4036.

Farina, K.L., Huttelmaier, S., Musunuru, K., Darnell, R., and Singer, R.H. 2003. Two ZBP1 KH domains facilitate β-actin mRNA localization, granule formation and cytoskeletal attachment. *J. Cell Biol.* **160:** 77–87.

Forristall, C., Pondel, M., Chen, L., and King, M. 1995. Patterns of localisation and cytoskeletal association of two vegetally localized RNAs, *Vg1* and *Xcat-2*. *Development* **121:** 201–208.

Geng, C. and Macdonald, P.M. 2006. Imp associates with squid and Hrp48 and contributes to localized expression of gurken in the oocyte. *Mol. Cell. Biol.* **26:** 9508–9516.

Git, A. and Standart, N. 2002. The KH domains of *Xenopus* Vg1RBP mediate RNA binding and self-association. *RNA* **8:** 1319–1333.

Gross, S.D., Schwab, M.S., Taieb, F.E., Lewellyn, A.L., Qian, Y.-W., and Maller, J.L. 2000. The critical role of the MAP kinase pathway in meiosis II in *Xenopus* oocytes is mediated by p90^{rsk}. *Curr. Biol.* **10:** 430–438.

Gross, S.D., Lewellyn, A.L., and Maller, J. 2001. A constitutively active form of the protein kinase p90[Rsk1] is sufficient to trigger the G2/M transition in *Xenopus* oocytes. *J. Biol. Chem.* **276:** 46099–46103.

Hammer, N.A., Hansen, T.O., Byskov, A.G., Rajpert-De Meyts, E., Grøndahl, M.L., Bredkjaer, H.E., Wewer, U.M., Christiansen, J., and Nielsen, F.C. 2005. Expression of IGF-II mRNA-binding proteins (IMPs) in gonads and testicular cancer. *Reproduction* **130:** 203–212.

Havin, L., Git, A., Elisha, Z., Oberman, F., Schwartz, S.P., Standart, N., and Yisraeli, J.K. 1998. RNA binding protein conserved in both microtubule and microfilament-based RNA localization. *Genes & Dev.* **12:** 1593–1598.

Huttelmaier, S., Zenklusen, D., Lederer, M., Dictenberg, J, Lorenz, M., Meng, X., Bassell, G.J., Condeelis, J., and Singer, R.H. 2005. Spatial regulation of β-actin translation by Src-dependent phosphorylation of ZBP1. *Nature* **438:** 512–515.

Iwasaki, T., Koretomo, Y., Fukuda, T., Paronetto, M.P., Sette, C., Fukami, Y., and Sato, K. 2008. Expression, phosphorylation, and mRNA-binding of heterogeneous nuclear ribonucleoprotein K in *Xenopus* oocytes, eggs, and early embryos. *Dev. Growth Differ.* **50:** 23–40.

King, M.L., Messitt, T.J., and Mowry, K.L. 2005. Putting RNAs in the right place at the right time: RNA localization in the frog oocyte. *Biol. Cell* **97:** 19–33.

Kobel, M., Weidensdorfer, D., Reinke, C., Lederer, M., Schmitt, W.D., Zeng, K., Thomssen, C., Hauptmann, S., and Huttelmaier, S. 2007. Expression of the RNA-binding protein IMP1 correlates with poor prognosis in ovarian carcinoma. *Oncogene* **26:** 7584–7589.

Kress, T.L., Yoon, Y.J., and Mowry, K.L. 2004. Nuclear RNP complex assembly initiates cytoplasmic RNA localization. *J. Cell Biol.* **165:** 203–211.

Kroll, T.T., Zhao, W., Jiang, C., and Huber, P.W. 2002. A homolog of FBP2/KSRP binds to localized mRNAs in *Xenopus* oocytes. *Development* **129:** 5609–5619.

Kwon, S., Abramson, T., Munro, T.P., John, C.M., Kohrmann, M., and Schnapp, B.J. 2002. UUCAC and Vera dependent localisation of VegT RNA in *Xenopus* oocytes. *Curr. Biol.* **12:** 558–564.

Leung, K.M., van Horck, F.P., Lin, A.C., Allison, R., Standart, N., and Holt, C.E. 2006. Asymmetrical β-actin mRNA translation in growth cones mediates attractive turning to netrin-1. *Nat. Neurosci.* **9:** 1247–1256.

Lewis, R.A., Gagnon, J.A., and Mowry, K.L. 2008. PTB/hnRNP I is required for RNP remodeling during RNA localization in *Xenopus* oocytes. *Mol. Cell. Biol.* **28:** 679–686.

Messias, A.C., Harnisch, C., Ostareck-Lederer, A., Sattler, M., and Ostareck, D.H. 2006. The DICE-binding activity of KH domain 3 of hnRNP K is affected by c-Src-mediated tyrosine phosphorylation. *J. Mol. Biol.* **361:** 470–481.

Munro, T.P., Kwon, S., Schnapp, B.J., and St Johnston, D. 2006. A repeated IMP-binding motif controls oskar mRNA translation and anchoring independently of *Drosophila melanogaster* IMP. *J. Cell Biol.* **172:** 577–588.

Nielsen, J., Christiansen, J., Lykke-Andersen, J., Johnsen, A.H., Wewer, U.M., and Nielsen, F.C. 1999. A family of insulin-like growth factor II mRNA-binding proteins represses translation in late development. *Mol. Cell. Biol.* **9:** 1262–1270.

Nielsen, J., Kristensen, M.A., Willemoes, M., Nielsen, F.C., and Christiansen, J. 2004. Sequential dimerization of human zipcode-binding protein IMP1 on RNA: A cooperative mechanism providing RNP stability. *Nucleic Acids Res.* **32:** 4368–4376.

Noubissi, F.K., Elcheva, I., Bhatia, N., Shakoori, A., Ougolkov, A., Liu, J., Minamoto, T., Ross, J., Fuchs, S.Y., and Spiegelman, V.S. 2006. CRD-BP mediates stabilization of βTrCP1 and c-myc mRNA in response to β-catenin signalling. *Nature* **441:** 898–901.

Ostareck-Lederer, A., Ostareck, D.H., Cans, C., Neubauer, G., Bomsztyk, K., Superti-Furga, G., and Hentze, M. 2002. c-Src-mediated phosphorylation of hnRNP K drives translational activation of specifically silenced mRNAs. *Mol. Cell. Biol.* **22:** 4535–4543.

Palmer, A. and Nebreda, A.R. 2000. The activation of MAP kinase and p34cdc2/cyclin B during the meiotic maturation of *Xenopus* oocytes. *Prog. Cell Cycle Res.* **4:** 131–143.

Palmer, A., Gavin, A.C., and Nebreda, A. 1998. A link between MAP kinase and p34[cdc2]/cyclin B during oocyte maturation: p90[rsk] phosphorylates and inactivates the p34[cdc2] inhibitory kinase Myt1. *EMBO J.* **17:** 5037–5047.

Perdiguero, E., Pillaire, M.J., Bodart, J.F., Hennersdorf, F., Frodin, M., Duesbery, N.S., Alonso, G., and Nebreda, A.R. 2003. Xp38γ/SAPK3 promotes meiotic G$_2$/M transition in *Xenopus* oocytes and activates Cdc25C. *EMBO J.* **22:** 5746–5756.

Pondel, M.D. and King, M.L. 1988. Localized maternal mRNA related to transforming growth factor β mRNA is concentrated in a cytokeratin-enriched fraction from *Xenopus* oocytes. *Proc. Natl. Acad. Sci.* **85:** 7612–7616.

Rand, K. and Yisraeli, J.K. 2007. Vg1 RNA localization in oocytes in the absence of xVICKZ3 RNA-binding activity. *Differentiation* **75:** 566–574.

Ross, A.F., Oleynikov, Y., Kislauskis, E.H., Taneja, K.L., and Singer, R.H. 1997. Characterization of a β-actin mRNA zipcode-binding protein. *Mol. Cell. Biol.* **17:** 2158–2165.

Shav-Tal, Y. and Singer, R.H. 2005. RNA localization. *J. Cell Sci.* **118:** 4077–4081.

Sohaskey, M.L. and Ferrell, J.E.J. 1999. Distinct, constitutively active MAPK phosphatases function in *Xenopus* oocytes: Implications for p42 MAPK regulation in vivo. *Mol. Biol. Cell* **10:** 3729–3743.

St Johnston, D. 2005. Moving messages: The intracellular localization of mRNAs. *Nat. Rev. Mol. Cell Biol.* **6:** 363–375.

Stohr, N., Lederer, M., Reinke, C., Meyer, S., Hatzfeld, M., Singer, R.H., and Huttelmaier, S. 2006. ZBP1 regulates mRNA stability during cellular stress. *J. Cell Biol.* **175:** 527–534.

Terasaki, M., Runft, L.L., and Hand, A.R. 2001. Changes in organization of the endoplasmic reticulum during *Xenopus* oocyte maturation and activation. *Mol. Biol. Cell* **12:** 1103–1116.

Vikesaa, J., Hansen, T.V., Jonson, L., Borup, R., Wewer, U.M., Christiansen, J., and Nielsen, F.C. 2006. RNA-binding IMPs promote cell adhesion and invadopodia formation. *EMBO J.* **25:** 1456–1468.

Weeks, D.L. and Melton, D.A. 1987. A maternal mRNA localized to the vegetal hemisphere in *Xenopus* eggs codes for a growth factor related to TGF-β. *Cell* **51:** 861–867.

Yaniv, K., Fainsod, A., Kalcheim, C., and Yisraeli, J.K. 2003. The RNA-binding protein Vg1 RBP is required for cell migration during early neural development. *Development* **130:** 5649–5661.

Yao, J., Sasaki, Y., Wen, Z., Bassell, G.J., and Zheng, J.Q. 2006. An essential role for β-actin mRNA localization and translation in Ca^{2+}-dependent growth cone guidance. *Nat. Neurosci.* **9:** 1265–1273.

Yisraeli, J.K. 2005. VICKZ proteins: A multi-talented family of regulatory RNA-binding proteins. *Biol. Cell* **97:** 87–96.

Yisraeli, J.K., Sokol, S., and Melton, D.A. 1990. A two-step model for the localization of maternal mRNA in *Xenopus* oocytes: Involvement of microtubules and microfilaments in the translocation and anchoring of Vg1 mRNA. *Development* **108:** 289–298.

Yoon, Y.J. and Mowry, K.L. 2004. *Xenopus* Staufen is a component of a ribonucleoprotein complex containing Vg1 RNA and kinesin. *Development* **131:** 3035–3045.

Zhang, H.L., Eom, T., Oleynikov, Y., Shenoy, S.M., Liebelt, D.A., Dictenberg, J.B., Singer, R.H., and Bassell, G.J. 2001. Neurotrophin-induced transport of a β-actin mRNP complex increases β-actin levels and stimulates growth cone motility. *Neuron* **31:** 261–275.

Zhao, W.M., Jiang, C., Kroll, T.T., and Huber, P. 2001. A proline-rich protein binds to the localization element of *Xenopus* Vg1 mRNA and to ligands involved in actin polymerization. *EMBO J.* **20:** 2315–2325.